The Influence of Interdomain Interactions on the Intradomain Motions in Yeast Phosphoglycerate Kinase: A Molecular Dynamics Study

Erika Balog,* Monique Laberge,*† and Judit Fidy*
*Department of Biophysics and Radiation Biology and Research Group for Membrane Biology of the Hungarian Academy of Sciences, Faculty of Medicine, Semmelweis University, Budapest, Hungary; and †Department of Biochemistry and Biophysics and Johnson Research Foundation, University of Pennsylvania Medical Center, Philadelphia, Pennsylvania 19104-6059

ABSTRACT A 3-ns molecular dynamics simulation in explicit solvent was performed to examine the inter- and intradomain motions of the two-domain enzyme yeast phosphoglycerate kinase without the presence of substrates. To elucidate contributions from individual domains, simulations were carried out on the complete enzyme as well as on each isolated domain. The enzyme is known to undergo a hinge-bending type of motion as it cycles from an open to a closed conformation to allow the phosphoryl transfer occur. Analysis of the correlation of atomic movements during the simulations confirms hinge bending in the nanosecond timescale: the two domains of the complete enzyme exhibit rigid body motions anticorrelated with respect to each other. The correlation of the intradomain motions of both domains converges, yielding a distinct correlation map in the enzyme. In the isolated domain simulations—in which interdomain interactions cannot occur—the correlation of domain motions no longer converges and shows a very small correlation during the same simulation time. This result points to the importance of interdomain contacts in the overall dynamics of the protein. The secondary structure elements responsible for interdomain contacts are also discussed.

INTRODUCTION

Phosphoglycerate kinase (PGK), a key enzyme in glycolysis, catalyzes the transfer of a phosphoryl group from 1,3-diphosphoglycerate (1,3-DPG) to adenosine diphosphate (ADP) to form 3-phosphoglycerate (3-PGA), and adenosine triphosphate (ATP). Crystallographic studies revealed that it is a monomeric two-domain enzyme with a binding site for 3-PGA at the N-terminal domain and with an ATP binding site at the C-terminal domain (1–4). The crystal structures determined for horse (5), yeast (2), pig muscle (3), and *Bacillus stearothermophilus* PGK (4) are very similar: they reveal two approximately same-sized domains, separated by a deep cleft, and linked by α-helix 5. Helices 13 and 14 of the C-terminal loop back to the N-domain (Fig. 1). Table 1 lists the amino acids of the different secondary structure elements in the molecule, and Table 2 lists the residues of the binding sites.

The two substrate-binding sites are rather far from each other (12–15 Å) to allow the phosphoryl transfer to occur. Thus it was suggested that upon binding of the two substrates to the open form of the enzyme, a hinge-bending motion converts the enzyme to a closed conformation to allow the reaction to occur (1). The first crystal structure of the closed conformation of PGK from *Trypanosoma brucei* in a ternary complex with Mg-ADP and 3-PGA was determined in 1997 (6). This structure showed a 32° hinge bending relative to the open conformation of unligated horse PGK (5). In this conformation, the two substrates are close enough to each other that in the absence of water, the phosphoryl transfer can occur. In the same year, the closed conformation of PGK from *Thermotoga maritima* was also reported (7). The structures determined by X-ray crystallography thus identified the two end states of the hinge-bending motion for several species but, to date, both open and closed conformations of PGK from the same species still remain to be crystallized (8).

For yeast PGK, computational studies attempted to predict the closed conformation starting from the available open structure determined by X-ray crystallography. Vaidehi et al., using a coarse-grained molecular dynamics (MD) method—treating the two domains as rigid bodies connected by a flexible hinge region (9)—were able to describe a large-scale domain motion that brings the substrates together. Using a path exploration with distance constraints (PEDC) method, which carries out MD simulations with root mean-square (RMS) distance constraints with respect to a reference structure, Guilbert et al. (10) proposed a closed structure for PGK in which the geometrical requirement for phosphoryl transfer was fulfilled. The same group also reported a normal mode analysis of the open structure of PGK, describing three types of motions, namely a twist propeller motion, a scissors-type hinge motion, and a shear motion between the domains (11). Moreover, they showed that modes of frequencies below 5 cm^{-1} contribute the most to the hinge-bending motions of the N- and C-terminal domains of the enzyme. As for experimental evidence, Haran et al. (12) reported time-resolved fluorescence measurements in substrate-free PGK, indicative of a large number of conformational substates in solution with slow interconversion on the nanosecond scale. The increase of the interdomain distance upon addition of substrate

Submitted July 12, 2006, and accepted for publication November 6, 2006.

Address reprint requests to Judit Fidy, Dept. of Biophysics and Radiation Biology, Faculty of Medicine, Semmelweis University, PO Box 263, H-1444 Budapest, Hungary. Tel.: 36-1-267-6261; Fax: 36-1-266-6656; E-mail: judit@puskin.sote.hu.

0006-3495/07/03/1709/08 $2.00

doi: 10.1529/biophysj.106.093195

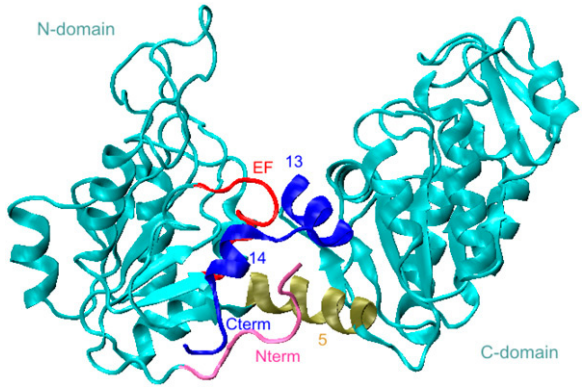

FIGURE 1 X-ray structure of yeast PGK. Numbers 5, 13, and 14 denote α-helices; EF denotes the loop.

was interpreted as a hinge-bending signature. Direct physical measurements of the characteristics of the PGK domain motion are, however, still lacking.

Since PGK is a two-domain enzyme, the role of interdomain interactions in the stability of the native state (13–16) and in protein folding (17–20) has been extensively studied experimentally. It was shown that both isolated domains can fold as independent units and that the interdomain contacts in the protein contribute relatively little to the stability of the folded ground state (15,21,22). However, interdomain interactions have recently been proposed to play a significant role in the kinetics of the PGK folding-unfolding pathways (23,24).

In this work, we used all-atom MD simulations and cross correlation analysis to describe the motions and the role of interdomain contacts in yeast PGK without substrates and in its isolated N- and C-domains. We selected this approach, i.e., comparing the dynamics of the three separate systems, to investigate the effect of interdomain interactions on the internal motions of the domains. Our results reveal that the rigid body type of hinge-bending motion can be clearly identified on a 3-ns timescale in yeast PGK without substrate, and the interdomain interactions significantly affect the intradomain motions of both domains. We also identified important details of the secondary structure elements that are responsible for the interdomain contacts.

TABLE 1 Secondary structure elements of yeast PGK. Numbers denote α-helices, letters denote β-sheets.

Residue number	Name	
17–21	A	
37–51	1	
57–59	B	
77–87	2	
91–94	C	N-domain
100–108	3	
113–116	D	
142–152	4	
157–159	E	
181–183	F	
185–199	5	
205–209	G	
217–226	6	
231–235	H	
237–243	7	
245–251	8	
257–273	9	
276–279	I	
282–286	J	C-domain
294–298	K	
315–325	10	
331–333	L	
348–359	11	
366–368	M	
372–380	12	
387–389	N	
393–401	13	
406–410	14	

TABLE 2 Residues of the substrate binding sites

Mg-ADP	3-PGA
Gly-371	Arg-38
Asp-372	Thr-391
Glu-341	Gly-392
Gly-211	Gly-393
Leu-311	Gly-394
Trp-308	
Asn-334	
Lys-213	
Lys-217	

METHODS

MD simulations were carried out on yeast PGK and its isolated N- [1–186] and C- [187–415] domains. The three systems were built from the crystallographic coordinates obtained from the Protein Data Bank, entry 3PGK.pdb (2). Since the crystal was not grown in the presence of the substrates but soaked in a solution containing the dissolved substrates to determine their binding sites, we considered the structure as that of substrate-free yeast PGK (25) and removed the ligands. The simulations were performed using CHARMM (26) version 31b2 with the all-atom-27 protein force field and NAMD2 (27). Positions for hydrogen atoms were generated using the HBUILD routine of CHARMM. The protein and its isolated domains were energy minimized in vacuum to eliminate unfavorable crystal interactions. Harmonic constraints were applied to heavy atoms to achieve smooth minimization. Using a steepest descent algorithm, the harmonic force constant was decreased every 500 steps from 10, 1, and 0.1 kcal/mol/Å^2, followed by 200 steps of a conjugate gradient algorithm with a 0.1 kcal/mol/Å^2 force constant. Unconstrained minimization was then applied for 100 steps with steepest descent and for 200 steps with a conjugate gradient method.

Whereas PGK has a net charge of zero, the N- and C-domains have a $+2$ and -2 charge, respectively. To achieve charge neutrality, two chloride ions were added randomly to the N-domain and two sodium ions to the C-domain. All three systems were immersed in a 300-K equilibrated TIP3 water box of 8-Å thickness in the x,y,z directions from the protein surface. Those TIP3 molecules that overlapped with either protein or counterions at a distance <2.8 Å were deleted. The primary unit cell was replicated using periodic boundary conditions. The solvated systems were energy minimized with progressively decreasing harmonic constraints as described above, followed by 2400 steps of unconstrained adopted basis Newton-Rapson method.

MD simulations were carried out with an integration time step of 0.001 ps and a dielectric constant set to 1. Electrostatic interactions were calculated using the particle mesh Ewald (PME) method (28) with a grid spacing of 1 Å or less and order of 4; the real space summation was truncated at 13.0 Å, and the width of the Gaussian distribution was set to 0.34 $Å^{-1}$ (29). Van der Waals interactions were reduced to zero by ''switch'' truncation operating from 10.0–12.0 Å. The energy-minimized structures were first heated to 300 K with a temperature increment of 10 K every 100 steps. The Hoover method (30) was used to equilibrate the system at constant temperature for 50 ps. Subsequently, a constant pressure and temperature (NPT) equilibration was applied for 250 ps. The Langevin piston method (31) was used to maintain the system at constant pressure with a piston temperature of 300 K, a damping coefficient of 5 ps^{-1}, a piston oscillation period of 200 fs, and a piston oscillation decay time of 100 fs. After the equilibration period, a 4-ns NPT production run was carried out and the coordinates of the trajectories were saved every 0.5 ps.

Pair correlations

The first nanosecond of the production run of PGK and of its isolated N- and C-domains was used to let the systems fully equilibrate. For cross correlation analysis, the last 3 ns of the production run were selected. The cross correlation matrix (C_{ij}) of the atomic displacements of atoms i and j is defined by $C_{ij} = \langle (r_i - \bar{r}_i)(r_j - \bar{r}_j) \rangle / \sqrt{\langle (r_i - \bar{r}_i)^2 (r_j - \bar{r}_j)^3 \rangle}$, where r_i and r_j are the positions and $\bar{r}_i$ and $\bar{r}_j$ are the mean positions of atoms i and j. The angular brackets denote time averages (32).

Since PGK is a two-domain enzyme, the conventional method of removing translations and rotations of the whole protein from the trajectories is not adequate. Therefore, to separate the inter- and intradomain motions of the two domains, the following approach was used: first each structure of the trajectory was transformed such that the C_α coordinates of the N-domain best fit the first trajectory frame of the N-domain. The cross correlation matrix and root mean-square deviation (RMSD) of C_α atoms were calculated after this transformation. This method yields the intradomain motion of the N-domain and shows the motion of the C-domain relative to the N-domain. A similar procedure was applied to the C-domain to see its intradomain motions and the motion of the N-domain relative to the C. For the separated N- and C-domains, the fitting was performed in the usual way, that is, onto their first structure of the analyzed trajectory, after which C_{ij} and RMSD were calculated.

RESULTS AND DISCUSSION

Overall behavior

Fig. 2 shows the average RMSD of backbone atoms of the structures along the MD trajectory using the energy-minimized crystal structures as reference for all three systems. The plots show that the structures of the separated N- and C-domains are stable during the studied timescale, whereas the RMSD of the whole protein exhibits an increasing tendency. To elucidate the reason for the increase in RMSD of PGK during the run, we calculated the distance between the center of mass of the two domains during the simulation time, which is shown in Fig. 3. The two centers of masses first depart from each other, and they start to get closer again after 2 ns. A very similar feature is observed when the radius of gyration (R_g) is plotted as a function of time. The value of R_g at the beginning of our simulation oscillates around 24.6 Å (data not shown), in good agreement with the value of 24.0 Å obtained by small angle neutron scattering

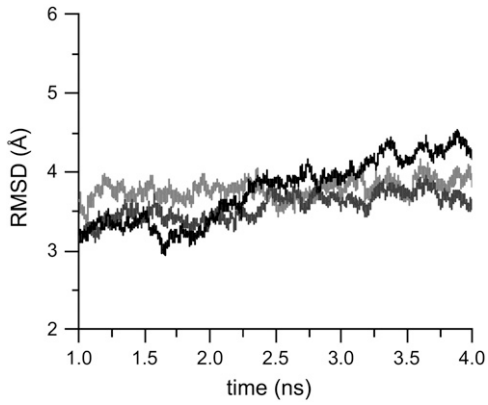

FIGURE 2 RMSD of backbone atoms between the energy-minimized crystal structure and trajectory snapshots during the last 3 ns of the production run for PGK (*black*), isolated N-domain (*light gray*), and isolated C-domain (*gray*).

(33). Following the same pattern as Fig. 3 when the domains depart from each other, R_g also increased to 25.9 Å. After this peak, the domains start to get closer again. In Fig. 4 we show snapshots from the production run at the beginning of the second, third, and fourth and at the end of the fourth nanosecond. To see the structures more clearly they are overlapped to the C-domain of the first structure. Both Fig. 3 and Fig. 4 indicate that the reason for the increase of protein RMSD compared to the energy-minimized crystal structure is the movement of the two domains relative to each other. These figures also indicate that longer simulations are needed to fully explore the rotation of the domains. This finding is in agreement with the experimental results indicating that this motion is out of the nanosecond timescale (12).

In Fig. 5 *a*, the average RMS fluctuations of C_α atoms of each residue during the analyzed 3-ns period are presented for all three systems. A general characteristic is that all of the systems exhibit the highest mobility in their loop regions. These deviations are relatively large, suggesting large structural fluctuation. Fig. 5 *b* shows the RMS fluctuation for

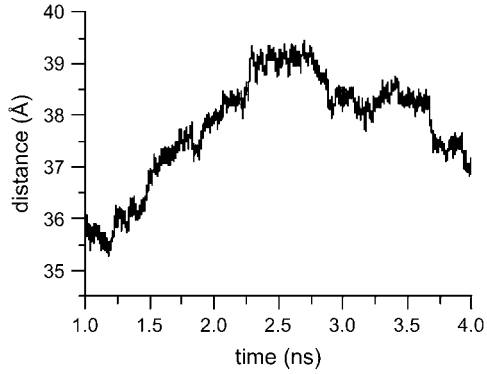

FIGURE 3 Distance between the center of mass of the two domains of PGK during the last 3 ns of the production run.

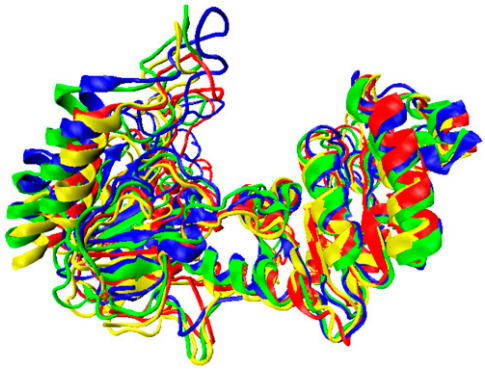

FIGURE 4 Snapshots of PKG at the beginning of the second (*red*), third (*yellow*), and fourth (*green*) and at the end of the fourth (*blue*) nanosecond of the simulation. The structures are superimposed on the C domain of the first structure.

residues after removing rigid body motions. For the whole protein, the RMS fluctuations of the N-domain were calculated after superposition to the first structure in the analyzed trajectory of the N-domain; the RMS fluctuations of the C-domain were calculated after doing the superposition to the first structure of the C-domain. As the figure shows, the loop movements of PGK and its isolated domains show very similar RMS fluctuations. By removing the rigid body motions it becomes even more pronounced that the loop regions in both PGK and in its isolated domains represent high RMS fluctuation values. We note displacements in the protein fluctuations that are in agreement with the normal mode studies of Guilbert et al. (11), namely for loops D4 and JK. It is noteworthy that helix 5 [187–199] in the protein—the region between the domains—also shows a fluctuation peak, whereas in the isolated C-domain (which starts with helix 5) this peak is not present. Fig. 6 shows the RMSD of helix 5 compared to helix 5 in the energy-minimized crystal structure. After ~1.8 ns, the RMSD of the helix in the protein increases from 0.4 to 1.5 Å, reaching another equilibrium state, whereas in the isolated C-domain, the RMSD is constant, fluctuating around ~0.8 Å. The change in the RMSD of the interdomain helix indicates that it changes its conformation compared to the original C-domain structure. The change in the conformation of the interdomain helix has also been reported by X-ray studies of *T. brucei* PGK (6), the interdomain helix acting as the hinge region.

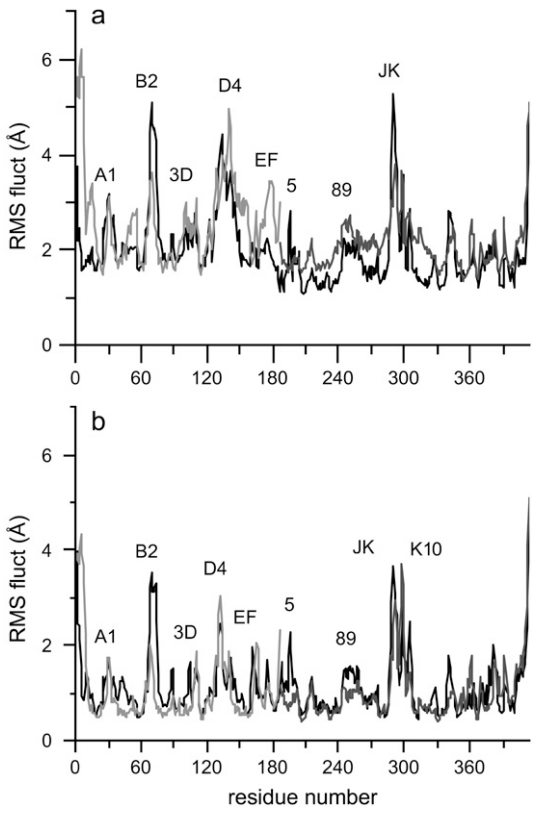

FIGURE 5 Average RMS fluctuations of the C_α atoms of each residue during the last 3 ns of the production run for PGK (*black*), isolated N-domain (*light gray*), isolated C-domain (*gray*) (*a*) from the original trajectory; (*b*) from the trajectory generated after removing the rigid-body domain motion. Loop regions are marked.

Domain motions

One way of identifying domain motions in a protein is by following the correlation of atomic motions (32,34,35). The magnitude of the correlation can be quantified by calculating the cross correlation coefficient between the atomic displacements (see Methods), which extends from +1 (atoms moving in the same direction) to −1 (atoms moving in the opposite directions). When C_{ij} is close to zero, the atomic motions are uncorrelated, and their movements are random compared to each other. The cross correlation matrix of the C_α atoms of PGK during the last 3 ns of the production run is presented in Fig. 7. In general, the data show that there is a positive correlation of the atomic movements within the two domains and anticorrelation in between the domain motions. This indicates that a good part of the amino acids within one

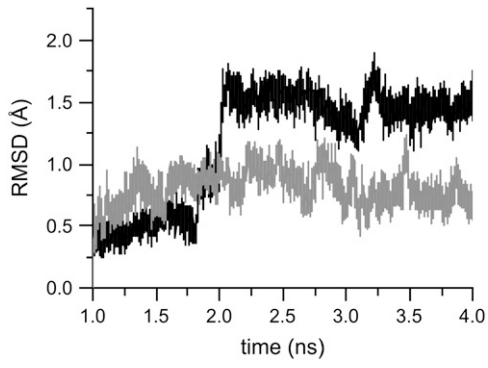

FIGURE 6 RMSD of helix 5 between the energy-minimized crystal structure and trajectory snapshots during the last 3 ns of the production run for PGK (*black*), isolated C-domain (*gray*).

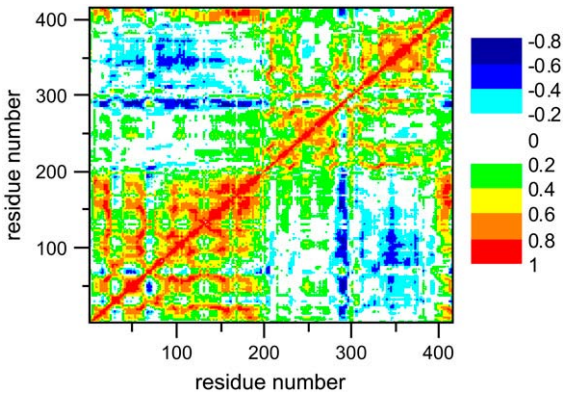

FIGURE 7 Cross correlation matrix of the atomic displacements of the C_α atoms in PGK. Red regions indicate that the C_α atoms move in the same direction (positive correlation), and blue regions indicate that they move in opposite directions (negative correlation).

domain move together but that the direction of the motion of the two domains is in the opposite sense. This type of motion is characteristic of 'hinge bending', as referred to in the PGK literature (11,36,37).

Before analyzing in detail the motions of the different structural elements, it is worth distinguishing between intradomain and interdomain motions present in Fig. 7. To do so, the cross correlation matrix of the C_α atoms was calculated in two ways. First, the PGK structure was superimposed on the first analyzed production run structure of the N-domain; second, the superposition was done on the first analyzed production run structure of the C-domain (see Methods). Fig. 8, *a* and *b*, shows the result of the calculations in these two cases. Above the diagonal, the cross correlation coefficients of the PGK C_α displacements are shown and below the diagonal the motions in the separated domains are represented. In Fig. 8 *a*, the right upper corner of the graph clearly demonstrates that the whole C-domain moves as a rigid body with very high correlation among its residues compared to the N-domain. This shows the motion of the C-domain with respect to the N, being an interdomain motion. The upper left corner of the graph shows that the first part of the EF loop [160–170] moves with a high positive correlation together with the main part of the C-domain and that several loops—namely, A1 [22–36], B2 [60–76], and D4 [133–148]—are anticorrelated with it. The lower left corner of the graph shows the intradomain motions within the N-domain. The N-domain in the protein is seen above the diagonal and the isolated N-domain below. In general, the N-domain in the protein shows a more structured intradomain motion pattern than the separated domain. To determine if the intradomain motions have converged during the simulation time (38,39), the cross correlation maps for different parts of the trajectory (first 2-ns and the entire 3-ns runs) were calculated. They show that the correlation coefficients of the N-domain in the protein have converged, whereas different correlation maps were obtained for the isolated N-domain, indicating that its intradomain motions have not converged during the studied timescale. Concerning the intradomain motions of the N-domain in the protein, we note that a positive correlation can be seen within the amino acids of the EF loop and that this loop shows anticorrelation with a good part of the N-domain. This suggests that it moves as a single dynamic unit within the N-domain.

Fig. 8 *b* shows the result of the calculations with superposition on the first analyzed production run structure of the C-domain. The lower left corner of the graph shows the interdomain motions of the N-domain relative to the C-domain. A similar type of interdomain motion can be observed as in Fig. 8 *a*: a movement with high positive correlation that extends to the entire N-domain. It is again a rigid-body-type movement of the N-domain compared to the C-domain. The upper left corner of the graph shows that the C-terminal of the protein [404–415] exhibits a high positive correlation with the N-domain. The existence of this movement is in agreement with earlier structural findings indicating that the C-terminal bends back to the N-domain (2,14,22). We note that an important part of the C-domain, namely the region in between the G and H sheets [205–235], JK loop [287–293], and the region between the L sheet and helix 12 [331–372], shows clear anticorrelated motion relative to the N-domain. The upper right corner of the graph shows the intradomain motions within the C-domain: the C-domain in the protein is above the diagonal, and the isolated C-domain correlation

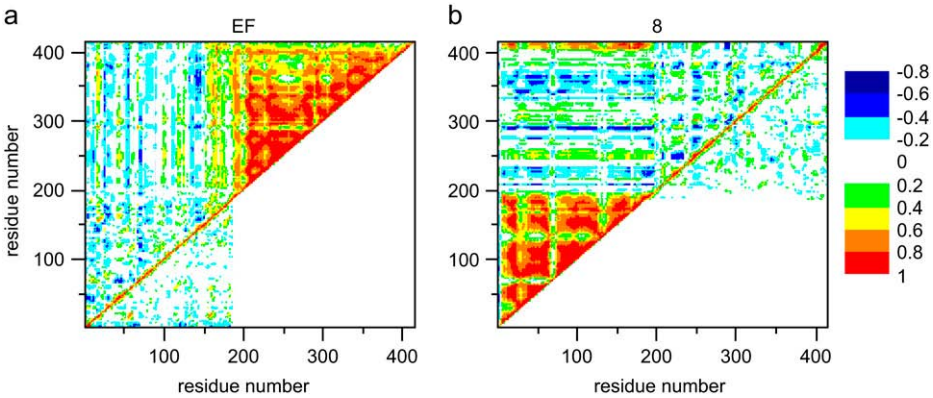

FIGURE 8 Cross correlation matrix of the atomic displacements of C_α atoms. PGK is represented above the diagonal, and the isolated N- and C-domain are below. Red regions indicate positive, blue regions indicate negative correlation. (*a*) With the rigid body motion of the N-domain removed. (*b*) With the rigid body motion of the C-domain removed.

coefficients are shown below. In general, the intradomain motion behavior of the C-domain is very similar compared to the N-domain: the C-domain in the protein shows more structured intradomain motion than its separated counterpart. Examination of the correlation maps at different simulation times shows that the correlation coefficients in the separated domain do not converge in the studied period, whereas the intradomain motions of the C-domain in the protein do converge during this time. We note that in the protein, helix 8 [244–253] shows anticorrelation with the C-domain and some positive correlation with the C-terminal of the protein [380–415] and the N-domain.

By comparing the intradomain motions of the two domains in the protein with the separated domains, we note that the atomic motions within the domains in the protein converge during the studied timescale and show a well-patterned correlation map. In the absence of the interdomain interactions, however, the intradomain motions do not converge and show weak correlation during the same time period. To locate which structural elements are close to each other (and whose interactions may account for the domain movements), we show in Fig. 9 the distance between the C_α atoms of each residue at the beginning of the 3-ns run. Above the diagonal, distances of C_α atoms in the protein are presented, and below the diagonal the distances for the separate domains are shown. Both the upper right and the lower left corner of the graph are symmetrical to the diagonal, meaning that there is no main structural difference between the protein and the separated domains. This is in agreement with the results of heteronuclear NMR spectroscopy, showing that the secondary structure of the isolated N-domain is identical with that of the intact protein (15). The upper left corner of the graph shows the distance between the atoms of the two domains of the protein. It can be seen that the C-terminal [390–415] bends back to the N-terminal [1–23]. The importance of this interaction has also been noted in the experimental work of Ritco-Vonsovici et al. (22), who studied the effect of C-terminal helix deletion on the folding of yeast PGK. The deletion increased the flexibility and decreased the stability of the folded protein. Fig. 9 also shows that the EF loop [156–180] of the N-domain is in close proximity to the C-terminal. The effect of this interdomain interaction can also be seen in the high correlation of the movement of the EF loop and the C-domain (Fig. 8 *a*). There are some other weaker contacts between sheet F, loop A1, helix 1, and loops B2 and D4 with the C-terminal, which may also play a role in interdomain interactions.

In many enzymes, domain motions and interdomain interactions are the object of increasing interest since domain closure is believed to bring the substrate together while facilitating the enzyme reaction. Both crystallographers (37) and theoreticians (40,41) have provided descriptions of interdomain motions and their structural basis. Among others, the Nussinov group has investigated the types of interactions present in available open and closed forms of hinge-bending proteins (42), noting from a structural perspective how the energetic penalty of opening the closed conformation is overcome by the absence of strong electrostatic interactions and salt bridges between domains. Hayward (41) also described the structural principles governing hinge-bending motions, proposing that α-helices store elastic energy to drive domain closure and substrate capture. But we are not aware of any experimental or theoretical work that discusses the effect of interdomain interaction on internal motion of the domains—and such is the contribution of our work.

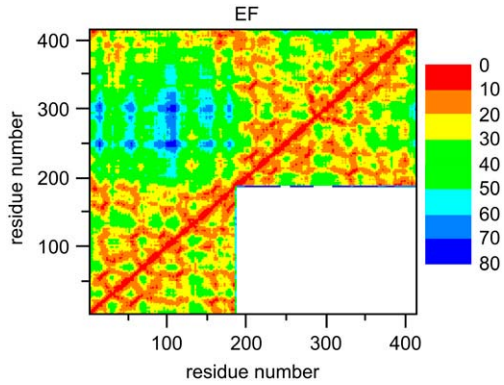

FIGURE 9 Distance map of C_α atoms in PGK. Red regions indicate C_α atoms that are closest to each other; blue indicate C_α atoms that are farthest compared to each other.

CONCLUSIONS

The analysis of the MD simulations which we performed on PGK and its isolated N- and C-domains allows us to distinguish between the interdomain and intradomain motions of the enzyme and to describe interdomain contacts. Our simulations confirm that the C-terminal bends back to the N-domain and interacts with the N-terminal. Our results also show that there is another secondary structure element that also plays a role in interdomain interactions: the EF loop of the N-domain. This loop is in proximity to helices 13 and 14 of the C-domain, and its motion is correlated with the motion of the helices. Analysis of the intradomain motions of the separated domains and of the intact protein shows that the atomic motions within the domains converge in the protein during the investigated timescale and show a well-defined correlation pattern—unlike the correlated motions of the separated domains, which do not converge and show a weak correlation pattern during the same time period. This effect is a clear signature of the presence or lack of interdomain interactions. Previous experimental work from our laboratory showed that the interdomain contacts in yeast PGK modify both the folding and the misfolding kinetics of the domains and that domain-domain interactions direct the folding of both domains in an asymmetric way (23,24). In this work, we gain insight in the direct role of the interdomain contacts in the conformational dynamics of the protein.

Our results also confirm the hinge-bending motion attributed to PGK, showing that, even on the nanosecond scale, the two domains of PGK move like rigid bodies in opposite phase relative to each other. These results are in agreement with earlier normal mode studies (11) demonstrating that the hinge-bending motion exists even without the substrates. Substrate binding is expected to affect this motion and modify the dynamics to reach a closed conformation. Further MD simulation studies to unravel this effect are in progress.

We thank David Perahia for useful discussions.

Financial support from the Hungarian Academy of Sciences (one-year fellowship, E.B.), from a Centre National de la Recherche Scientifique, France-Hungarian Academy of Sciences collaborative grant, and from the Hungarian grant No. 512/2006 of the Scientific Committee of the Ministry of Health, Hungary, (J.F.) is highly appreciated.

REFERENCES

1. Banks, R. D., C. C. Blake, P. R. Evans, R. Haser, D. W. Rice, G. W. Hardy, M. Merrett, and A. W. Phillips. 1979. Sequence, structure and activity of phosphoglycerate kinase: a possible hinge-bending enzyme. *Nature*. 279:773–777.
2. Watson, H. C., N. P. C. Walker, P. J. Shaw, T. N. Bryant, P. L. Wemdell, L. A. Fothergill, R. E. Perkins, S. C. Conroy, M. J. Dobson, M. F. Tuite, A. J. Kingsman, and S. M. Kingsman. 1982. Sequence and structure of yeast phosphoglycerate kinase. The EMBO J. 1:1635–1640.
3. Harlos, K., M. Vas, and C. F. Blake. 1992. Crystal structure of the binary complex of pig muscle phosphoglycerate kinase and its substrate 3-phospho-D-glycerate. *Proteins*. 12:133–144.
4. Davies, G. J., S. J. Gamblin, J. A. Littlechid, Z. Dauter, K. S. Wilson, and H. C. Watson. 1994. The structure of a thermally stable 2 3-phosphoglycerate kinase and a comparison with its mesophilic equivalent. *Acta Crystallogr. D*. 50:202–209.
5. Blake, C. C., and P. R. Evans. 1974. Structure of horse muscle phosphoglycerate kinase. Some results on the chain conformation, substrate binding and evolution of the molecule from a 3 angstrom Fourier map. *J. Mol. Biol*. 84:585–601.
6. Bernstein, B. E., P. A. Michels, and W. G. Hol. 1997. Synergistic effects of substrate-induced conformational changes in phosphoglycerate kinase activation. *Nature*. 385:275–278.
7. Auerbach, G., R. Huber, M. Grattinger, K. Zaiss, H. Schurig, R. Jaenicke, and U. Jacob. 1997. Closed structure of phosphoglycerate kinase from Thermotoga maritima reveals the catalytic mechanism and determinants of thermal stability. *Structure*. 5:1475–1483.
8. Kovari, Z., and M. Vas. 2004. Protein conformer selection by sequence-dependent packing contacts in crystals of 3-phosphoglycerate kinase. *Proteins*. 55:198–209.
9. Vaidehi, N., and W. A. I. Goddard. 2000. Domain motions in phosphoglycerate kinase using hierarchical NEIMO molecular dynamics simulations. *J. Phys. Chem. A*. 104:2375–2383.
10. Guilbert, C., D. Perahia, and L. Mouawad. 1995. A method to explore transition paths in macromolecules. Applications to hemoglobin and phosphoglycerate kinase. *Comput. Phys. Comm.* 91:263–273.
11. Guilbert, C., F. Pecorari, D. Perahia, and L. Mouawad. 1996. Low frequency motions in phosphoglycerate kinase. A normal mode analysis. *Chem. Phys.* 204:324–336.
12. Haran, G., E. Haas, B. K. Szpikowska, and M. T. Mas. 1992. Domain motions in phosphoglycerate kinase: determination of interdomain distance distributions by site-specific labeling and time-resolved fluorescence energy transfer. *Proc. Natl. Acad. Sci. USA*. 89:11764–11768.
13. Adams, B., R. Fowler, M. Hudson, and R. H. Pain. 1996. The role of the C-terminal lysine in the hinge bending mechanism of yeast phosphoglycerate kinase. *FEBS Lett*. 385:101–104.
14. Mas, M. T., H. H. Chen, K. Aisaka, L. N. Lin, and J. F. Brandts. 1995. Effects of C-terminal deletions on the conformational state and denaturation of phosphoglycerate kinase. *Biochemistry*. 34:7931–7940.
15. Hosszu, L. L., C. J. Craven, J. Spencer, M. J. Parker, A. R. Clarke, M. Kelly, and J. P. Waltho. 1997. Is the structure of the N-domain of phosphoglycerate kinase affected by isolation from the intact molecule? *Biochemistry*. 36:333–340.
16. Minard, P., L. Hall, J. M. Betton, D. Missiakas, and J. M. Yon. 1989. Efficient expression and characterization of isolated structural domains of yeast phosphoglycerate kinase generated by site-directed mutagenesis. *Protein Eng*. 3:55–60.
17. Missiakas, D., J. M. Betton, P. Minard, and J. M. Yon. 1990. Unfolding-refolding of the domains in yeast phosphoglycerate kinase: comparison with the isolated engineered domains. *Biochemistry*. 29: 8683–8689.
18. Pecorari, F., C. Guilbert, P. Minard, M. Desmadril, and J. M. Yon. 1996. Folding and functional complementation of engineered fragments from yeast phosphoglycerate kinase. *Biochemistry*. 35:3465–3476.
19. Hosszu, L. L., C. J. Craven, M. J. Parker, M. Lorch, J. Spencer, A. R. Clarke, and J. P. Waltho. 1997. Structure of a kinetic protein folding intermediate by equilibrium amide exchange. *Nat. Struct. Biol*. 4:801–804.
20. Szilagyi, A. N., and M. Vas. 1998. Sequential domain refolding of pig muscle 3-phosphoglycerate kinase: kinetic analysis of reactivation. *Fold. Des*. 3:565–575.
21. Parker, M. J., J. Spencer, G. S. Jackson, S. G. Burston, L. L. Hosszu, C. J. Craven, J. P. Waltho, and A. R. Clarke. 1996. Domain behavior during the folding of a thermostable phosphoglycerate kinase. *Biochemistry*. 35:15740–15752.
22. Ritco-Vonsovici, M., B. Mouratou, P. Minard, M. Desmadril, J. M. Yon, M. Andrieux, E. Leroy, and E. Guittet. 1995. Role of the C-terminal helix in the folding and stability of yeast phosphoglycerate kinase. *Biochemistry*. 34:833–841.
23. Osvath, S., G. Kohler, P. Zavodszky, and J. Fidy. 2005. Asymmetric effect of domain interactions on the kinetics of folding in yeast phosphoglycerate kinase. *Protein Sci*. 14:1609–1616.
24. Osvath, S., M. Jackel, G. Agocs, P. Zavodszky, G. Kohler, and J. Fidy. 2006. Domain interactions direct misfolding and amyloid formation of yeast phosphoglycerate kinase. *Proteins*. 62:909–917.
25. Varga, A., B. Flachner, E. Graczer, S. Osvath, A. N. Szilagyi, and M. Vas. 2005. Correlation between conformational stability of the ternary enzyme-substrate complex and domain closure of 3-phosphoglycerate kinase. *FEBS J*. 272:1867–1885.
26. Brooks, B. R., R. E. Bruccoleri, B. D. Olafson, D. J. States, S. Swaminathan, and M. Karplus. 1983. CHARMM: a program for macromolecular energy, minimization and dynamics calculations. *J. Comput. Chem*. 4:187–217.
27. Phillips, J. C., R. Braun, W. Wang, J. Gumbart, E. Tajkhorshid, E. Villa, C. Chipot, R. D. Skeel, L. Kale, and K. Schulten. 2005. Scalable molecular dynamics with NAMD. *J. Comput. Chem*. 26:1781–1802.
28. Luty, B. A., M. E. Davis, I. G. Tironi, and F. Van Gunsteren. 1994. A comparison of particle-particle, particle-mesh and Ewald methods for calculating electrostatic interactions. *Mol. Simul*. 14:11–20.
29. Yang, C., G. S. Jas, and K. Kuczera. 2001. Structure and dynamics of calcium-activated calmodulin in solution. *J. Biomol. Struct. Dyn*. 19: 247–271.
30. Hoover, W. G. 1985. Canonical dynamics: equilibrium phase-space distributions. *Phys. Rev. A*. 31:1695–1697.
31. Feller, S. E., Y. Zhang, R. W. Pastor, and B. R. Brooks. 1995. Constant pressure molecular dynamics simulation: the Langevin piston method. *J. Chem. Phys*. 103:4613–4621.
32. Ichiye, T., and M. Karplus. 1991. Collective motions in proteins: a covariance analysis of atomic fluctuations in molecular dynamics and normal mode simulations. *Proteins*. 11:205–217.
33. Henderson, S. J., E. H. Serpersu, B. S. Gerhardt, and G. J. Bunick. 1994. Conformational changes in yeast phosphoglycerate kinase upon substrate binding. *Biophys. Chem*. 53:95–104.

34. Rod, T. H., J. L. Radkiewicz, and C. L. Brooks 3rd. 2003. Correlated motion and the effect of distal mutations in dihydrofolate reductase. *Proc. Natl. Acad. Sci. USA.* 100:6980–6985.

35. Verma, C. S., L. S. Caves, R. E. Hubbard, and G. C. Roberts. 1997. Domain motions in dihydrofolate reductase: a molecular dynamics study. *J. Mol. Biol.* 266:776–796.

36. Blake, C. 1997. Phosphotransfer hinges in PGK. *Nature*. 385:204–205.

37. Gerstein, M., A. M. Lesk, and C. Chothia. 1994. Structural mechanisms for domain movements in proteins. *Biochemistry*. 33:6739–6749.

38. Radkiewicz, J. L., and C. L. Brooks III. 2000. Protein dynamics in enzymatic catalysis: exploration of dihydrofolate reductase. *J. Am. Chem. Soc.* 122:225–231.

39. Hunenberger, P. H., A. E. Mark, and W. F. van Gunsteren. 1995. Fluctuation and cross-correlation analysis of protein motions observed in nanosecond molecular dynamics simulations. *J. Mol. Biol.* 252: 492–503.

40. Hayward, S., and H. J. Berendsen. 1998. Systematic analysis of domain motions in proteins from conformational change: new results on citrate synthase and T4 lysozyme. *Proteins.* 30:144–154.

41. Hayward, S. 1999. Structural principles governing domain motions in proteins. *Proteins*. 36:425–435.

42. Sinha, N., S. Kumar, and R. Nussinov. 2001. Interdomain interactions in hinge-bending transitions. *Structure*. 9:1165–1181.